Journal of Zhejiang University SCIENCE A
ISSN 1673-565X (Print); ISSN 1862-1775 (Online)
www.zju.edu.cn/jzus; www.springerlink.com
E-mail: jzus@zju.edu.cn

A generalized trajectory tracking controller for robot manipulators with bounded inputs*

Hua-shan LIU†, Shi-qiang ZHU
(*State Key Lab of Fluid Power Transmission and Control, Zhejiang University, Hangzhou 310027, China*)
†E-mail: watson683@163.com

Received Oct. 18, 2008; Revision accepted Apr. 4, 2009; Crosschecked Aug. 14, 2009

Abstract: A generalized controller based on stability theory of singularly perturbed systems is proposed, to deal with the problem of bounded actuator inputs in robot trajectory tracking control. The saturation function with error-gain matrix is applied in the torque control law, which ensures the upper bound of torque inputs in any given limited range. Through appropriately setting the entries of the error-gain matrix, the tracking performance can be improved. Moreover, a pseudo signal is generated from a linear filter to substitute for the actual velocity error, eliminating the need for velocity measurements. Finally, to verify the effectiveness of the generalized controller, a new saturated controller with error-gain-contained arc tangent function is designed. Comparison experiments show that the proposed controller can strictly guarantee the bound of the torque inputs in situations with non-zero initial tracking errors, and gives a better tracking result than other controllers.

Key words: Robot, Tracking control, Singular perturbation, Bounded input
doi:10.1631/jzus.A0820725 **Document code:** A **CLC number:** TP24

INTRODUCTION

The limited power of actuators has been ignored in previous designs of robot controllers. The majority of control strategies were designed on the basis of actuators offering the arbitrarily large torque required (Paden and Panja, 1988; Loria and Ortega, 1995; de Queiroz *et al*., 1997; Reyes and Kelly, 2001). Recently, researchers have begun to take into account the problem of bounded torque inputs. Solutions have been created mostly by using hyperbolic tangent functions to ensure the upper bound, but most of them are targeted at the set-point control (Kelly *et al*., 1997; Santibanez *et al*., 1998; Laib, 2000; Zavala-Rio and Santibanez, 2006).

Velocity and acceleration measurements can easily be disturbed by noise signals, and in some situations where the measurements are not available to deal with these problems, tracking controllers with only position measurements and bounded torque inputs have been proposed. The first tracking controller with bounded torque inputs was designed by Loria and Nijmeijer (1998). The hyperbolic tangent function was applied in the tracking control law to guarantee the upper bound of torque input in the permitted range. A pseudo velocity error signal was obtained through a nonlinear filter that contained only the information of the actual position tracking error, ensuring control of the whole closed-loop without velocity and acceleration measurements. Dixon *et al*. (1999) proposed a new output feedback tracking controller with bounded torque inputs, similar to that described by Loria and Nijmeijer (1998), which yielded semi-global stability in closed loop. Santibanez and Kelly (2001) designed a torque-bounded controller that considered the viscous friction at the robot joint, and proposed that if the viscous friction damping is large enough, the global asymptotic stability of the system is guaranteed. Along with Moreno-Valenzuela *et al*.(2008b), they showed that applying appropriate extra gains in the hyperbolic

* Project (No. 2008C21106) supported by the Zhejiang Provincial Science and Technology Foundation of China

tangent saturation functions can improve tracking performance. The stability theory of singularly perturbed systems was used to give an explicit proof of the system stability. Moreno-Valenzuela *et al*.(2008a) presented a class of output feedback controllers in an attempt to generalize the results of Loria and Nijmeijer (1998), but it added a restriction on velocity error while using the singular perturbation theory.

In this paper, a new generalized controller with an error-gain matrix in the saturation function of the control law and only joint position measurements in the whole closed-loop control is proposed, based on stability theory of singularly perturbed systems. Taking it as a template, a new sample controller with modified arc tangent saturation function is designed to make comparisons with two other controllers, to verify the effectiveness of the proposed generalized controller.

Notations: In this paper, we use $\|\cdot\|$ for either Euclidean norm of vectors or induced L_2 norm of matrices. $|\cdot|_m$ and $\|\cdot\|_m$ denote the minimum and $|\cdot|_M$ and $\|\cdot\|_M$ the maximum values of $|\cdot|$ and $\|\cdot\|$, respectively. $\lambda_m\{\}$ stands for the smallest and $\lambda_M\{\}$ for the largest eigenvalues of matrices.

DYNAMIC MODEL AND PROPERTIES

The dynamics of a rigid serial n-link robot manipulator with revolute joints can be written as

$$\boldsymbol{M}(\boldsymbol{q})\ddot{\boldsymbol{q}}+\boldsymbol{C}(\boldsymbol{q},\dot{\boldsymbol{q}})\dot{\boldsymbol{q}}+\boldsymbol{G}(\boldsymbol{q})+\boldsymbol{F}_{\mathrm{v}}\dot{\boldsymbol{q}}=\boldsymbol{\tau}, \tag{1}$$

where $\boldsymbol{q}\in\mathbb{R}^n$ denotes the joint angle vector, $\boldsymbol{M}(\boldsymbol{q})\in\mathbb{R}^{n\times n}$ the inertia matrix, $\boldsymbol{C}(\boldsymbol{q},\dot{\boldsymbol{q}})\in\mathbb{R}^{n\times n}$ the centripetal-Coriolis matrix, $\boldsymbol{G}(\boldsymbol{q})\in\mathbb{R}^n$ the gravity effect, $\boldsymbol{F}_{\mathrm{v}}=\mathrm{diag}\{f_{\mathrm{v}1}, f_{\mathrm{v}2}, \ldots, f_{\mathrm{v}n}\}\in\mathbb{R}^{n\times n}$ ($f_{\mathrm{v}i}>0$, $i=1, 2, \ldots, n$) the viscous friction coefficient matrix, and $\boldsymbol{\tau}\in\mathbb{R}^n$ the input torque vector.

Some useful properties are listed as follows (Loria and Nijmeijer, 1998; Kelly *et al*., 2005; Moreno-Valenzuela *et al*., 2008b):

Property 1 The inertia and centripetal-Coriolis matrices satisfy the following skew symmetric relationship:

$$\boldsymbol{x}^{\mathrm{T}}[\dot{\boldsymbol{M}}(\boldsymbol{q})-2\boldsymbol{C}(\boldsymbol{q},\dot{\boldsymbol{q}})]\boldsymbol{x}=0, \tag{2}$$

$$\dot{\boldsymbol{M}}(\boldsymbol{q})=\boldsymbol{C}(\boldsymbol{q},\dot{\boldsymbol{q}})+\boldsymbol{C}(\boldsymbol{q},\dot{\boldsymbol{q}})^{\mathrm{T}}. \tag{3}$$

Property 2 The inertia matrix $\boldsymbol{M}(\boldsymbol{q})$ is symmetric, positive definite, and satisfies the following inequalities:

$$\lambda_{\mathrm{m}}\{\boldsymbol{M}(\boldsymbol{q})\}\|\boldsymbol{x}\|^2\le\boldsymbol{x}^{\mathrm{T}}\boldsymbol{M}(\boldsymbol{q})\boldsymbol{x}\le\lambda_{\mathrm{M}}\{\boldsymbol{M}(\boldsymbol{q})\}\|\boldsymbol{x}\|^2. \tag{4}$$

Property 3 $\forall\boldsymbol{x}, \boldsymbol{y}, \boldsymbol{z}\in\mathbb{R}^n$, the centripetal-Coriolis matrix satisfies the following transformations:

$$\boldsymbol{C}(\boldsymbol{x},\boldsymbol{y})\boldsymbol{z}=\boldsymbol{C}(\boldsymbol{x},\boldsymbol{z})\boldsymbol{y}, \tag{5}$$

$$\boldsymbol{C}(\boldsymbol{x},\boldsymbol{y}+\boldsymbol{z})=\boldsymbol{C}(\boldsymbol{x},\boldsymbol{y})+\boldsymbol{C}(\boldsymbol{x},\boldsymbol{z}). \tag{6}$$

Property 4 The centripetal-Coriolis, gravity terms can be bounded in the following manner:

$$\|\boldsymbol{C}(\boldsymbol{q},\dot{\boldsymbol{q}})\|\le k_{\mathrm{C}}\|\dot{\boldsymbol{q}}\|,\quad \|\boldsymbol{G}(\boldsymbol{q})\|_{\mathrm{M}}\le k_{\mathrm{G}}. \tag{7}$$

GENERALIZED CONTROLLER

In this section, we will first give the control goal, then introduce a class of saturation functions, and finally, develop a generalized position output feedback tracking controller with bounded inputs.

Control goal

The control objective was to design a controller with bounded inputs $|\tau_i|<\tau_{i\mathrm{M}}$, $i=1, 2, \ldots, n$, which guarantees the joint displacements $\boldsymbol{q}(t)\in\mathbb{R}^n$ converge asymptotically to the desired joint displacements $\boldsymbol{q}_{\mathrm{d}}(t)\in\mathbb{R}^n$, where τ_i denotes the control torque input of the ith joint, and correspondingly, $\tau_{i\mathrm{M}}$ denotes the permitted maximum torque input of the ith joint.

We define the position tracking error $\boldsymbol{e}(t)\in\mathbb{R}^n$ as

$$\boldsymbol{e}(t)=\boldsymbol{q}_{\mathrm{d}}(t)-\boldsymbol{q}(t). \tag{8}$$

Assume $\boldsymbol{q}_{\mathrm{d}}(t)$ and its first two time derivatives are bounded:

$$\|\boldsymbol{q}_{\mathrm{d}}(t)\|\le\|\boldsymbol{q}_{\mathrm{d}}(t)\|_{\mathrm{M}},\ \|\dot{\boldsymbol{q}}_{\mathrm{d}}(t)\|\le\|\dot{\boldsymbol{q}}_{\mathrm{d}}(t)\|_{\mathrm{M}},\ \|\ddot{\boldsymbol{q}}_{\mathrm{d}}(t)\|\le\|\ddot{\boldsymbol{q}}_{\mathrm{d}}(t)\|_{\mathrm{M}}. \tag{9}$$

Then, the control goal can be expressed as

$$\forall\boldsymbol{e}(0)\in\mathbb{R}^n,\quad \lim_{t\to\infty}\boldsymbol{e}(t)=\boldsymbol{0}. \tag{10}$$

A class of saturation functions

To ensure the upper bound of absolute value of torque input, an appropriate saturation function should be applied in the control law. Following Moreno-Valenzuela *et al*.(2008a), we have found a class of more generalized saturation functions with the following properties:

We define $\mathrm{Sat}(\boldsymbol{x}, \boldsymbol{\Delta})=[\mathrm{sat}(x_1, \sigma_1), \mathrm{sat}(x_2, \sigma_2), \ldots, \mathrm{sat}(x_n, \sigma_n)]^{\mathrm{T}}$, where $\boldsymbol{x}=[x_1, x_2, \ldots, x_n]^{\mathrm{T}}\in\mathbb{R}^n$, $\boldsymbol{\Delta}=\mathrm{diag}\{\sigma_1, \sigma_2, \ldots, \sigma_n\}\in\mathbb{R}^{n\times n}$, $\sigma_i\geq1$, $i=1, 2, \ldots, n$. Here, we use σ_{m} and σ_{M} to represent the minimum and the maximum values of σ_i, respectively.

i) $\mathrm{sat}(x_i, \sigma_i)$ is a monotone increasing function, i.e., $\dfrac{\partial \mathrm{sat}(x_i,\sigma_i)}{\partial x_i}>0$, $\forall x_i\in\mathbb{R}$.

ii) $\mathrm{sat}(x_i, \sigma_i)x_i\geq0$; if and only if $x_i=0$ and $\mathrm{sat}(x_i, \sigma_i)=0$, $\mathrm{sat}(x_i, \sigma_i)x_i=0$, $\forall x_i\in\mathbb{R}$.

iii) $|\mathrm{sat}(x_i, \sigma_i)|\leq p$, $\|\mathrm{Sat}(\boldsymbol{x},\boldsymbol{\Delta})\|\leq\sqrt{n}p$, $\forall x_i\in\mathbb{R}$, $\boldsymbol{x}\in\mathbb{R}^n$.

iv) $\sigma_{\mathrm{M}}\|\boldsymbol{x}\|\geq\alpha_1\|\mathrm{Sat}(\boldsymbol{x}, \boldsymbol{\Delta})\|$, $\forall\boldsymbol{x}\in\mathbb{R}^n$, where $\alpha_1>0$ is small enough.

v) $\mathrm{Sat}(\boldsymbol{x}, \boldsymbol{\Delta})$ is continuously differentiable and satisfies $\lambda_{\mathrm{M}}\left\{\dfrac{\partial\mathrm{Sat}(\boldsymbol{x},\boldsymbol{\Delta})}{\boldsymbol{\Delta}\partial\boldsymbol{x}}\right\}\leq\beta$, $\beta>0$ for all $\boldsymbol{x}\in\mathbb{R}^n$.

vi) $\alpha_2>0$ is always large enough such that for all $\boldsymbol{x}\in\Omega_\eta$, $\Omega_\eta=\{\boldsymbol{x}\in\mathbb{R}^n: \|\boldsymbol{x}\|\leq\eta\}$, where $\eta>0$ is arbitrarily large, $\sigma_{\mathrm{m}}\|\boldsymbol{x}\|\leq\alpha_2\|\mathrm{Sat}(\boldsymbol{x}, \boldsymbol{\Delta})\|$ is satisfied.

vii) For all $\boldsymbol{x}\in\Omega_\eta$, there exists small enough $\gamma_1>0$ and large enough $\gamma_2>0$ to satisfy $\gamma_1\|\mathrm{Sat}(\boldsymbol{x},\boldsymbol{\Delta})\|^2\leq\sum_{i=1}^{n}\sigma_i\int_0^{x_i}\mathrm{sat}(x_i,\sigma_i)\mathrm{d}x_i\leq\gamma_2\|\mathrm{Sat}(\boldsymbol{x},\boldsymbol{\Delta})\|^2$.

With the properties described above, the improvements compared with Moreno-Valenzuela *et al*.(2008a) can be summarized: we apply an extra positive gain σ_i that can change the approaching behavior to saturation of the function $\mathrm{sat}(x_i, \sigma_i)$, and we define a generalized relationship more than multiplication and division between x_i and σ_i.

Implementation of generalized controller

When tracking control without velocity measurements, we use a linear filter which can generate a pseudo signal $\boldsymbol{\xi}$ from only the position tracking error $\boldsymbol{e}$, to surrogate the actual velocity tracking error $\dot{\boldsymbol{e}}$. The filter is given as

$$\dot{\boldsymbol{r}}=\boldsymbol{U}\boldsymbol{\xi}, \tag{11}$$

$$\boldsymbol{\xi}=\boldsymbol{U}\boldsymbol{e}-\boldsymbol{r}, \tag{12}$$

where $\boldsymbol{r}\in\mathbb{R}^n$ is an auxiliary variable introduced to divide the overall filter into two implementable parts, and $\boldsymbol{\xi}$ is the output of the filter, $\boldsymbol{U}=\mathrm{diag}\{\mu_1, \mu_2, \ldots, \mu_n\}\in\mathbb{R}^{n\times n}$, $\mu_i>0$, $i=1, 2, \ldots, n$.

From Eqs.(11) and (12), we obtain

$$\dot{\boldsymbol{\xi}}=\boldsymbol{U}(\dot{\boldsymbol{e}}-\boldsymbol{\xi}). \tag{13}$$

To facilitate the expressions, we use $\boldsymbol{M}$, $\boldsymbol{C}$, $\boldsymbol{C}_{\mathrm{d}}$ and $\boldsymbol{G}$ to represent $\boldsymbol{M}(\boldsymbol{q})$, $\boldsymbol{C}(\boldsymbol{q}, \dot{\boldsymbol{q}})$, $\boldsymbol{C}(\boldsymbol{q}, \dot{\boldsymbol{q}}_{\mathrm{d}})$ and $\boldsymbol{G}(\boldsymbol{q})$, respectively. Then, we propose the generalized controller as

$$\begin{aligned}\boldsymbol{\tau}&=\boldsymbol{M}\ddot{\boldsymbol{q}}_{\mathrm{d}}+\boldsymbol{C}_{\mathrm{d}}\dot{\boldsymbol{q}}_{\mathrm{d}}+\boldsymbol{G}+\boldsymbol{F}_{\mathrm{v}}\dot{\boldsymbol{q}}_{\mathrm{d}}+\boldsymbol{K}_{\mathrm{p}}\mathrm{Sat}(\boldsymbol{e},\boldsymbol{K}_{\boldsymbol{e}})\\&\quad+\boldsymbol{K}_{\mathrm{d}}\mathrm{Sat}(\boldsymbol{\xi},\boldsymbol{K}_{\xi}),\end{aligned} \tag{14}$$

where $\boldsymbol{K}_{\mathrm{p}}=\mathrm{diag}\{k_{\mathrm{p}1}, k_{\mathrm{p}2}, \ldots, k_{\mathrm{p}n}\}$, $\boldsymbol{K}_{\mathrm{d}}=\mathrm{diag}\{k_{\mathrm{d}1}, k_{\mathrm{d}2}, \ldots, k_{\mathrm{d}n}\}\in\mathbb{R}^{n\times n}$; $\boldsymbol{K}_{\boldsymbol{e}}=\mathrm{diag}\{k_{\boldsymbol{e}1}, k_{\boldsymbol{e}2}, \ldots, k_{\boldsymbol{e}n}\}$, $\boldsymbol{K}_{\xi}=\mathrm{diag}\{k_{\xi1}, k_{\xi2}, \ldots, k_{\xi n}\}\in\mathbb{R}^{n\times n}$, and $k_{\mathrm{p}i}$, $k_{\mathrm{d}i}>0$, $k_{\boldsymbol{e}i}$, $k_{\xi i}\geq1$, for $i=1, 2, \ldots, n$.

Moreover, from Eq.(14), Properties 2, 4, iii), and Eq.(9), we can obtain

$$\begin{aligned}|\tau_i|_{\mathrm{M}}&\leq\|\boldsymbol{M}_i\|_{\mathrm{M}}\|\ddot{\boldsymbol{q}}_{\mathrm{d}}\|_{\mathrm{M}}+\|\boldsymbol{C}_{\mathrm{d}i}\|_{\mathrm{M}}\|\dot{\boldsymbol{q}}_{\mathrm{d}}\|_{\mathrm{M}}\\&\quad+|G_i|_{\mathrm{M}}+f_{\mathrm{v}i}|\dot{q}_{\mathrm{d}i}|_{\mathrm{M}}+(k_{\mathrm{p}i}+k_{\mathrm{d}i})p,\end{aligned} \tag{15}$$

where $\boldsymbol{M}_i$, $\boldsymbol{C}_{\mathrm{d}i}$ and G_i denote the ith row of $\boldsymbol{M}$, $\boldsymbol{C}_{\mathrm{d}}$ and $\boldsymbol{G}$, respectively. To follow the input constraints $|\tau_i|<\tau_{i\mathrm{M}}$, the following inequality should be satisfied:

$$\begin{aligned}\tau_{i\mathrm{M}}&>\|\boldsymbol{M}_i\|_{\mathrm{M}}\|\ddot{\boldsymbol{q}}_{\mathrm{d}}\|_{\mathrm{M}}+\|\boldsymbol{C}_{\mathrm{d}i}\|_{\mathrm{M}}\|\dot{\boldsymbol{q}}_{\mathrm{d}}\|_{\mathrm{M}}\\&\quad+|G_i|_{\mathrm{M}}+f_{\mathrm{v}i}|\dot{q}_{\mathrm{d}i}|_{\mathrm{M}}+(k_{\mathrm{p}i}+k_{\mathrm{d}i})p.\end{aligned} \tag{16}$$

SYSTEM STABILITY

In this section, a new method for analyzing the stability of the tracking control system is introduced. Based on the new method, we give the strict but brief stability proof of the generalized controller.

Theorem 1 Consider the nonlinear singularly per turbed system:

$$\dot{\boldsymbol{x}} = f(t, \boldsymbol{x}, \boldsymbol{z}, \varepsilon), \quad (17)$$

$$\varepsilon\dot{\boldsymbol{z}} = g(t, \boldsymbol{x}, \boldsymbol{z}, \varepsilon), \quad (18)$$

where $\boldsymbol{x}\in\mathbb{R}^{n_1}$, $\boldsymbol{z}\in\mathbb{R}^{n_2}$, $\varepsilon>0$. Assume that the assumptions below are satisfied $\forall(t, \boldsymbol{x}, \varepsilon)\in[0, +\infty)\times B_\eta\times[0, \varepsilon_0]$, $B_\eta=\{\boldsymbol{x}\in\mathbb{R}^{n_1}: \|\boldsymbol{x}\|\le\eta\}$:

1. $f(t, \mathbf{0}, \mathbf{0}, \varepsilon)=\mathbf{0}$ and $g(t, \mathbf{0}, \mathbf{0}, \varepsilon)=\mathbf{0}$.

2. The equation $g(t, \boldsymbol{x}, \boldsymbol{z}, \varepsilon)=\mathbf{0}$ has an isolated root $\boldsymbol{z}=h(t, \boldsymbol{x})$ such that $h(t, \mathbf{0})=\mathbf{0}$.

3. The functions f, g, h and their partial derivatives up to the second order are bounded for $\boldsymbol{z}-h(t, \boldsymbol{x})\in B_\rho$, where $B_\rho=\{\boldsymbol{x}\in\mathbb{R}^{n_2}: \|\boldsymbol{x}\|\le\rho\}$.

4. The origin of the reduced system

$$\dot{\boldsymbol{x}} = f(t, \boldsymbol{x}, h(t, \boldsymbol{x}), 0) \quad (19)$$

is exponentially stable.

5. The origin of the boundary-layer system

$$\frac{\mathrm{d}\boldsymbol{y}}{\mathrm{d}\delta} = g(t, \boldsymbol{x}, \boldsymbol{y} + h(t, \boldsymbol{x}), 0) \quad (20)$$

is exponentially stable, uniformly in $(t, \boldsymbol{x})$, where $\delta=t/\varepsilon$, and $\boldsymbol{y}=\boldsymbol{z}-h(t, \boldsymbol{x})$.

Then, there exists $\varepsilon^*>0$ such that for all $\varepsilon^*>\varepsilon$, the origin of Eqs.(18) and (19) is exponentially stable (Khalil, 2007).

Define $\boldsymbol{x}=[\boldsymbol{e}^{\mathrm{T}}\ \dot{\boldsymbol{e}}^{\mathrm{T}}]^{\mathrm{T}}$, $\boldsymbol{z}=\boldsymbol{\xi}$ and $\varepsilon=1/\mu$ (for convenience, we select $\mu_i=\mu$ in $\boldsymbol{U}$, i=1, 2, …, n), and substitute Eqs.(8) and (14) into Eq.(1), to obtain forms similar to Eqs.(17) and (18) by invoking Property 3:

$$\dot{\boldsymbol{x}}_1 = \dot{\boldsymbol{e}}, \quad (21)$$

$$\begin{aligned}\dot{\boldsymbol{x}}_2 = \ddot{\boldsymbol{e}} = -\boldsymbol{M}^{-1}[(\boldsymbol{C}+\boldsymbol{C}_{\mathrm{d}}+\boldsymbol{F}_{\mathrm{v}})\dot{\boldsymbol{e}} \\ +\boldsymbol{K}_{\mathrm{p}}\mathrm{Sat}(\boldsymbol{e}, \boldsymbol{K}_{\boldsymbol{e}})+\boldsymbol{K}_{\mathrm{d}}\mathrm{Sat}(\boldsymbol{\xi}, \boldsymbol{K}_{\xi})],\end{aligned} \quad (22)$$

$$\varepsilon\dot{\boldsymbol{z}} = \varepsilon\frac{\mathrm{d}\boldsymbol{\xi}}{\mathrm{d}t} = \dot{\boldsymbol{e}} - \boldsymbol{\xi}. \quad (23)$$

Substituting $\boldsymbol{\xi}=\dot{\boldsymbol{e}}$ into Eq.(22), we can obtain

$$\begin{aligned}\dot{\boldsymbol{x}}_2 = \ddot{\boldsymbol{e}} = -\boldsymbol{M}^{-1}[(\boldsymbol{C}+\boldsymbol{C}_{\mathrm{d}}+\boldsymbol{F}_{\mathrm{v}})\dot{\boldsymbol{e}} \\ +\boldsymbol{K}_{\mathrm{p}}\mathrm{Sat}(\boldsymbol{e}, \boldsymbol{K}_{\boldsymbol{e}})+\boldsymbol{K}_{\mathrm{d}}\mathrm{Sat}(\dot{\boldsymbol{e}}, \boldsymbol{K}_{\xi})].\end{aligned} \quad (24)$$

Then, Eqs.(21) and (24) build up the reduced system (slow model). Let $t/\varepsilon=\delta$. We can obtain the boundary-layer system (fast model) as follows:

$$\frac{\mathrm{d}\boldsymbol{y}}{\mathrm{d}\delta} = \frac{\mathrm{d}(\boldsymbol{\xi}-\dot{\boldsymbol{e}})}{\mathrm{d}\delta} = \frac{\mathrm{d}\boldsymbol{\xi}}{\mathrm{d}\delta} = \dot{\boldsymbol{e}} - \boldsymbol{\xi}, \quad (25)$$

where $\dot{\boldsymbol{e}}$ is recognized as a constant for the scaled time variable δ.

Proposition 1 For any $\left[\boldsymbol{e}(0)^{\mathrm{T}}\ \dot{\boldsymbol{e}}(0)^{\mathrm{T}}\ \boldsymbol{\xi}(0)^{\mathrm{T}}\right]^{\mathrm{T}} \in \Phi_\eta$, where $\Phi_\eta=\{\boldsymbol{x}\in\mathbb{R}^{3n}: \|\boldsymbol{x}\|\le\eta\}$, $\eta>0$ is arbitrarily large, if

$$k_{\mathrm{dm}}\left(\frac{\alpha_1}{k_{\xi\mathrm{M}}}\right)+f_{\mathrm{vm}}\left(\frac{\alpha_1}{k_{\xi\mathrm{M}}}\right)^2-k_{\mathrm{C}}\|\dot{\boldsymbol{q}}_{\mathrm{d}}\|_{\mathrm{M}}\left(\frac{\alpha_2}{k_{\xi\mathrm{m}}}\right)^2>0 \quad (26)$$

is satisfied, there always exists $\varepsilon^*>0$, and for all $\varepsilon^*>\varepsilon$, the state space origin of the system Eqs.(21)~(23) is exponentially stable.

Proof According to Theorem 1, if the singularly perturbed system Eqs.(21)~(23) satisfies all the assumptions 1~5, then the exponential stability can be achieved. Five steps are presented in sequence, as follows:

Step 1: From Eqs.(21)~(23), we can obtain $[\dot{\boldsymbol{e}}^{\mathrm{T}}\ \ddot{\boldsymbol{e}}^{\mathrm{T}}\ \dot{\boldsymbol{\xi}}^{\mathrm{T}}]^{\mathrm{T}}=[\mathbf{0}\ \mathbf{0}\ \mathbf{0}]^{\mathrm{T}}$, when $[\boldsymbol{e}^{\mathrm{T}}\ \dot{\boldsymbol{e}}^{\mathrm{T}}\ \boldsymbol{\xi}^{\mathrm{T}}]^{\mathrm{T}}=[\mathbf{0}\ \mathbf{0}\ \mathbf{0}]^{\mathrm{T}}$. So Assumption 1 is satisfied.

Step 2: Note that, when $\varepsilon=0$, we can obtain the unique isolated root of Eq.(23): $\boldsymbol{\xi}=\dot{\boldsymbol{e}}$.

In contrast to the generalized controller proposed by Moreno-Valenzuela *et al*.(2008a), the isolated root is $\mathrm{Sat}(\boldsymbol{\xi})=\dot{\boldsymbol{e}}$ (where Sat() is a class of saturation functions defined by the authors), which creates a bound to $\dot{\boldsymbol{e}}$. This may cause a serious decrease in the radius η with the too strict constraint condition $|\dot{e}_i|\le p$. This results from applying a nonlinear filter described as Eqs.(15) and (16) (Moreno-Valenzuela *et al*., 2008a).

Step 3: Determine that the right sides of Eqs.(21)~(23) have bounded partial derivatives up to the second order for $\boldsymbol{\xi}-\dot{\boldsymbol{e}}\in\boldsymbol{B}_\rho$.

Step 4: The state space origin $[\boldsymbol{e}^{\mathrm{T}}\ \dot{\boldsymbol{e}}^{\mathrm{T}}]^{\mathrm{T}}=\mathbf{0}$ is the only equilibrium point of the reduced system Eqs.(21) and (24). We define a Lyapunov function $V(t, \boldsymbol{e}, \dot{\boldsymbol{e}})$, written as V for short, as

$$V=\sum_{i=1}^{n}k_{\mathrm{p}i}\int_0^{e_i}\mathrm{sat}(e_i, k_{ei})\mathrm{d}e_i+\frac{1}{2}\dot{\boldsymbol{e}}^{\mathrm{T}}\boldsymbol{M}\dot{\boldsymbol{e}}+\upsilon\dot{\boldsymbol{e}}^{\mathrm{T}}\boldsymbol{M}\mathrm{Sat}(\boldsymbol{e}, \boldsymbol{K}_{\boldsymbol{e}}), \quad (27)$$

where constant $\upsilon>0$ is small enough.

Applying Properties 2 and vii), we obtain the inequality

$$V \ge \gamma_1 \left(\frac{k_{\mathrm{p}i}}{k_{ei}}\right)_{\mathrm{m}} \|\mathrm{Sat}(\boldsymbol{e},\boldsymbol{K}_{\boldsymbol{e}})\|^2 + \frac{1}{2}\lambda_{\mathrm{m}}\{\boldsymbol{M}\}\|\dot{\boldsymbol{e}}\|^2 - \upsilon\lambda_M\{\boldsymbol{M}\}\|\dot{\boldsymbol{e}}\|\,\|\mathrm{Sat}(\boldsymbol{e},\boldsymbol{K}_{\boldsymbol{e}})\|. \tag{28}$$

Therefore, it can be shown that, $\forall [\boldsymbol{e}^{\mathrm{T}}\ \dot{\boldsymbol{e}}^{\mathrm{T}}]^{\mathrm{T}} \in B_\eta$, V is positive definite under the condition

$$\upsilon < \upsilon_1 = \sqrt{2\gamma_1\lambda_{\mathrm{m}}\{\boldsymbol{M}\}\left(\frac{k_{\mathrm{p}i}}{k_{ei}}\right)_{\mathrm{m}}} \Big/ \lambda_{\mathrm{M}}\{\boldsymbol{M}\}.$$

After taking the time derivative of Eq.(27), substituting Eq.(22) for $\ddot{\boldsymbol{e}}$ and applying Property 1, we can obtain

$$\begin{aligned}\dot{V} = &-\dot{\boldsymbol{e}}^{\mathrm{T}}\left[(\boldsymbol{C}_{\mathrm{d}}+\boldsymbol{F}_{\mathrm{v}})\dot{\boldsymbol{e}} + \boldsymbol{K}_{\mathrm{d}}\mathrm{Sat}(\dot{\boldsymbol{e}},\boldsymbol{K}_\xi)\right] \\ &+\upsilon\Bigg[\ddot{\boldsymbol{e}}^{\mathrm{T}}\boldsymbol{M}\mathrm{Sat}(\boldsymbol{e},\boldsymbol{K}_{\boldsymbol{e}}) + \dot{\boldsymbol{e}}^{\mathrm{T}}\dot{\boldsymbol{M}}\mathrm{Sat}(\boldsymbol{e},\boldsymbol{K}_{\boldsymbol{e}}) \\ &+\dot{\boldsymbol{e}}^{\mathrm{T}}\boldsymbol{M}\frac{\partial \mathrm{Sat}(\boldsymbol{e},\boldsymbol{K}_{e})}{\partial \boldsymbol{e}}\dot{\boldsymbol{e}}\Bigg].\end{aligned} \tag{29}$$

Furthermore, using Properties 1~3, i)~vii) and the inequality $\|\dot{\boldsymbol{q}}\| \le \|\dot{\boldsymbol{e}}\| + \|\dot{\boldsymbol{q}}_{\mathrm{d}}\|$, we obtain

$$\begin{aligned}\dot{V} \le &-s_{11}\|\mathrm{Sat}(\boldsymbol{e},\boldsymbol{K}_{\boldsymbol{e}})\|^2 - s_{22}\|\mathrm{Sat}(\dot{\boldsymbol{e}},\boldsymbol{K}_\xi)\|^2 \\ &-(s_{12}+s_{21})\|\mathrm{Sat}(\boldsymbol{e},\boldsymbol{K}_{\boldsymbol{e}})\|\|\mathrm{Sat}(\dot{\boldsymbol{e}},\boldsymbol{K}_\xi)\|,\end{aligned} \tag{30}$$

where

$s_{11}=\upsilon k_{\mathrm{pm}}$, $s_{22}=T_1-\upsilon T_2$, $s_{12}=s_{21}=-\upsilon T_3$,

$$T_1 = k_{\mathrm{dm}}\left(\frac{\alpha_1}{k_{\xi\mathrm{M}}}\right) + f_{\mathrm{vm}}\left(\frac{\alpha_1}{k_{\xi\mathrm{M}}}\right)^2 - k_{\mathrm{C}}\|\dot{\boldsymbol{q}}_{\mathrm{d}}\|_{\mathrm{M}}\left(\frac{\alpha_2}{k_{\xi\mathrm{m}}}\right)^2,$$

$$T_2 = \left(\sqrt{n}pk_{\mathrm{C}} + \beta k_{e\mathrm{M}}\lambda_{\mathrm{M}}\{\boldsymbol{M}\}\right)\left(\frac{\alpha_2}{k_{\xi\mathrm{m}}}\right),$$

$$T_3 = \left(k_{\mathrm{C}}\|\dot{\boldsymbol{q}}_{\mathrm{d}}\|_{\mathrm{M}} + \frac{1}{2}f_{\mathrm{vM}}\right)\left(\frac{\alpha_2}{k_{\xi\mathrm{m}}}\right) + \frac{1}{2}k_{\mathrm{dM}}.$$

Then from Eq.(30), we can obtain the following form by transformation:

$$\begin{aligned}\dot{V} &\le -\begin{bmatrix}\|\mathrm{Sat}(\boldsymbol{e},\boldsymbol{K}_{\boldsymbol{e}})\| \\ \|\mathrm{Sat}(\dot{\boldsymbol{e}},\boldsymbol{K}_\xi)\|\end{bmatrix}^{\mathrm{T}} \boldsymbol{S} \begin{bmatrix}\|\mathrm{Sat}(\boldsymbol{e},\boldsymbol{K}_{\boldsymbol{e}})\| \\ \|\mathrm{Sat}(\dot{\boldsymbol{e}},\boldsymbol{K}_\xi)\|\end{bmatrix} \\ &\le -\lambda_{\mathrm{m}}\{\boldsymbol{S}\}\left\|\left[\|\mathrm{Sat}(\boldsymbol{e},\boldsymbol{K}_{\boldsymbol{e}})\|\ \ \|\mathrm{Sat}(\dot{\boldsymbol{e}},\boldsymbol{K}_\xi)\|\right]^{\mathrm{T}}\right\|^2,\end{aligned} \tag{31}$$

where the matrix $\boldsymbol{S} = \begin{bmatrix} s_{11} & s_{12} \\ s_{21} & s_{22}\end{bmatrix}$. It can be shown that the right-hand side of Eq.(31) will be negative definite if $\boldsymbol{S}$ is positive definite.

Note that $s_{11}=\upsilon k_{\mathrm{pm}}>0$. According to Sylvester's theorem, to ensure the matrix $\boldsymbol{S}$ positive definite, it should satisfy $s_{11}s_{22} - s_{12}^2 > 0$, i.e.,

$$\upsilon\left[k_{\mathrm{pm}}T_1 - \upsilon\left(k_{\mathrm{pm}}T_2 + T_3^2\right)\right] > 0, \tag{32}$$

where we already have $\upsilon>0$ and $k_{\mathrm{pm}}T_2 + T_3^2 > 0$.

If $\upsilon < \upsilon_2 = k_{\mathrm{pm}}T_1 \big/ \left(k_{\mathrm{pm}}T_2 + T_3^2\right)$ and $T_1>0$ (i.e., Eq.(26) is satisfied), $\boldsymbol{S}$ will be positive definite, then for all $[\boldsymbol{e}^{\mathrm{T}}\ \dot{\boldsymbol{e}}^{\mathrm{T}}]^{\mathrm{T}} \in B_\eta$, $\dot{V}$ will be negative definite, which implies the local asymptotic stability of the state space origin of the reduced system Eqs.(21) and (24).

In addition, we can obtain the inequality

$$\begin{aligned}V \le &\ \gamma_2\left(\frac{k_{\mathrm{p}i}}{k_{ei}}\right)_{\mathrm{M}}\|\mathrm{Sat}(\boldsymbol{e},\boldsymbol{K}_{\boldsymbol{e}})\|^2 \\ &+\frac{1}{2}\lambda_{\mathrm{M}}\{\boldsymbol{M}\}\left(\frac{\alpha_2}{k_{\xi\mathrm{m}}}\right)^2\|\mathrm{Sat}(\dot{\boldsymbol{e}},\boldsymbol{K}_\xi)\|^2 \\ &+\upsilon\lambda_{\mathrm{M}}\{\boldsymbol{M}\}\frac{\alpha_2}{k_{\xi\mathrm{m}}}\|\mathrm{Sat}(\dot{\boldsymbol{e}},\boldsymbol{K}_\xi)\|\|\mathrm{Sat}(\boldsymbol{e},\boldsymbol{K}_{\boldsymbol{e}})\|\end{aligned} \tag{33}$$

using Properties 2, vi), and vii).

Similarly, we can obtain the same form as described by Eq.(31):

$$\begin{aligned}V &\le \begin{bmatrix}\|\mathrm{Sat}(\boldsymbol{e},\boldsymbol{K}_{\boldsymbol{e}})\| \\ \|\mathrm{Sat}(\dot{\boldsymbol{e}},\boldsymbol{K}_\xi)\|\end{bmatrix}^{\mathrm{T}} \boldsymbol{Q} \begin{bmatrix}\|\mathrm{Sat}(\boldsymbol{e},\boldsymbol{K}_{\boldsymbol{e}})\| \\ \|\mathrm{Sat}(\dot{\boldsymbol{e}},\boldsymbol{K}_\xi)\|\end{bmatrix} \\ &\le \lambda_{\mathrm{M}}\{\boldsymbol{Q}\}\left\|\left[\|\mathrm{Sat}(\boldsymbol{e},\boldsymbol{K}_{\boldsymbol{e}})\|\ \ \|\mathrm{Sat}(\dot{\boldsymbol{e}},\boldsymbol{K}_\xi)\|\right]^{\mathrm{T}}\right\|^2,\end{aligned} \tag{34}$$

where $\boldsymbol{Q}\in\mathbb{R}^{n\times n}$ is a symmetric matrix.

From Eqs.(31) and (34), we can obtain

$$\dot{V} \le -\frac{\lambda_{\rm m}\{\boldsymbol{S}\}}{\lambda_{\rm M}\{\boldsymbol{Q}\}}V, \tag{35}$$

which indicates the exponential stability of the reduced system for all $[\boldsymbol{e}^{\rm T}\ \dot{\boldsymbol{e}}^{\rm T}]^{\rm T} \in B_\eta$. Note that the υ in V and $\dot{V}$ should satisfy $0<\upsilon<\min\{\upsilon_1, \upsilon_2\}$.

Step 5: For the boundary-layer system Eq.(25), we define a Lyapunov function $W(\delta, \boldsymbol{\xi})$, written as W for short, as

$$W = \omega(\dot{\boldsymbol{e}} - \boldsymbol{\xi})^2, \tag{36}$$

where constant $\omega>0$ is small enough. Then, we obtain

$$\frac{{\rm d}W}{{\rm d}\delta} = -2\omega(\dot{\boldsymbol{e}} - \boldsymbol{\xi})^2 = -2W, \tag{37}$$

which shows that the exponential stability of the boundary-layer system holds uniformly in $(t, \boldsymbol{x})$ without any restrictions on the initial state conditions. Also, we find that the exponential convergence rate increases as the scaled time variable $\delta=t/\varepsilon$ increases; i.e., the smaller the ε, the faster the exponential convergence of the boundary-layer system.

Therefore, according to Theorem 1, there always exists $\varepsilon^*>0$ satisfying condition $\varepsilon^*>\varepsilon$, such that for all $[\boldsymbol{e}(0)^{\rm T}\ \dot{\boldsymbol{e}}(0)^{\rm T}\ \xi(0)^{\rm T}]^{\rm T} \in \Phi_\eta$, the space origin of the system Eqs.(21)~(23) is exponentially stable.

SAMPLE CONTROLLER

The controllers referred to by Loria and Nijmeijer (1998) and Moreno-Valenzuela *et al*.(2008b) are two particular cases of the proposed generalized controller in this paper. The saturation function of Moreno-Valenzuela *et al*.(2008b) is chosen as the hyperbolic tangent function, with the relationship between x_i and σ_i of $sat(x_i, \sigma_i)$ selected as multiplication, i.e., $\tanh(\sigma_i, x_i)$, which satisfies Properties i)~vii). In Loria and Nijmejer (1998), the error gain σ_i in $\text{sat}(x_i, \sigma_i)$ turns out to be 1.

Based on the proposed generalized controller, we can design bounded controllers conveniently and flexibly using the following two steps:

Step 1: Divide the whole control system into two sub-systems (reduced system and boundary-layer system), and then design each sub-system separately.

Step 2: Design the proper saturation functions, which need only to satisfy Properties i)~vii), without any restrictions on the relationship between x_i and σ_i of $\text{sat}(x_i, \sigma_i)$.

Using this method, we design a new controller:

$$\begin{aligned}\boldsymbol{\tau} = &\boldsymbol{M}\ddot{\boldsymbol{q}}_{\rm d} + \boldsymbol{C}_{\rm d}\dot{\boldsymbol{q}}_{\rm d} + \boldsymbol{G} + \boldsymbol{F}_{\rm v}\dot{\boldsymbol{q}}_{\rm d}\\ &+ \boldsymbol{K}_{\rm p}{\rm Atan}(\boldsymbol{e}, \boldsymbol{K}_{\boldsymbol{e}}) + \boldsymbol{K}_{\rm d}{\rm Atan}(\boldsymbol{\xi}, \boldsymbol{K}_{\xi}),\end{aligned} \tag{38}$$

where $\boldsymbol{e}$ and $\boldsymbol{\xi}$ satisfy Eq.(13); $\text{Atan}(\boldsymbol{e}, \boldsymbol{K}_{\boldsymbol{e}})=[\text{atan}(e_1, k_{e1}), \text{atan}(e_2, k_{e2}), \ldots, \text{atan}(e_n, k_{en})]^{\rm T}$, $\text{Atan}(\boldsymbol{\xi}, \boldsymbol{K}_{\xi})=[\text{atan}(\xi_1, k_{\xi1}), \text{atan}(\xi_2, k_{\xi2}), \ldots, \text{atan}(\xi_n, k_{\xi n})]^{\rm T}$, $\text{atan}(e_i, k_{ei})$ and $\text{atan}(\xi_i, k_{\xi i})$ denote the arctangent functions $\arctan(k_{ei}e_i)$ and $\arctan(k_{\xi i}\xi_i)$, respectively, $i=1, 2, \ldots, n$; i.e., the $\text{sat}(x_i, \sigma_i)$ in the generalized tracking controller is designed as $\arctan(\sigma_i x_i)$.

Obviously, $\arctan(\sigma_i x_i)$ satisfies the properties i) and ii), and we can obtain $p=\pi/2$, $\alpha_1=1$, $\beta=1$ from the properties iii)~v) separately.

In Property vi), $\sigma_{\rm m}|x_i|/|\arctan(\sigma_i x_i)| \le \alpha_{2i}$, $\forall|x_i|\le\eta$, $i=1, 2, \ldots, n$. We obtain

$$\alpha_2 = \max\{\alpha_{21}, \alpha_{22}, \ldots, \alpha_{2n}\} = \sigma_{\rm m}\eta / \arctan(\sigma_{\rm m}\eta).$$

In Property vii), $\forall|x_i|\le\eta$, $i=1, 2, \ldots, n$,

$$\sigma_i\int_0^{x_i}\arctan(\sigma_i x_i){\rm d}x_i = \sigma_i x_i\arctan(\sigma_i x_i) - \frac{1}{2}\ln[1+(\sigma_i x_i)^2],$$

$$\gamma_{1i} \le \lim_{\sigma_i x_i \to 0}\frac{\sigma_i\eta\arctan(\sigma_i x_i) - \frac{1}{2}\ln[1+(\sigma_i x_i)^2]}{[\arctan(\sigma_i x_i)]^2} = \frac{1}{2},$$

so γ_1 can be selected as $\gamma_1=0.5$. On the other side, we have

$$\gamma_{2i} \ge \frac{\sigma_i\eta\arctan(\sigma_i\eta) - \frac{1}{2}\ln[1+(\sigma_i\eta)^2]}{[\arctan(\sigma_i\eta)]^2},$$

where γ_2 can be selected as $\gamma_2=\max\{\gamma_{21}, \gamma_{22}, \ldots, \gamma_{2n}\}$, i.e.,

$$\gamma_2 = \frac{\sigma_{\rm M}\eta\arctan(\sigma_{\rm M}\eta) - \frac{1}{2}\ln[1+(\sigma_{\rm M}\eta)^2]}{[\arctan(\sigma_{\rm M}\eta)]^2}.$$

Fig.1 shows the function curves of arctan($\sigma_i x_i$) for σ_i=1, 3, 10 and tanh x_i.

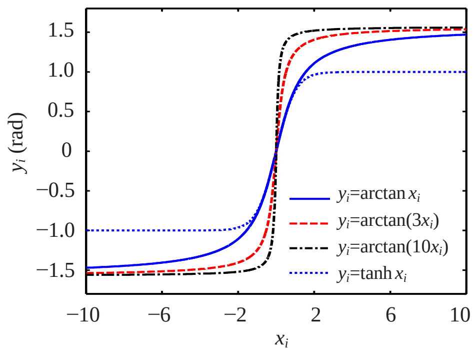

Fig.1 Function curves of arctan($\sigma_i x_i$) and tanh x_i

In response to increasing values of σ_i, the zero-crossing slope of function arctan($\sigma_i x_i$) increases steeply and rapidly approaches saturation. Function arctan() has a wider range of (−π/2, π/2) than function tanh() (with a range of (−1, 1)), resulting in a more moderate approach to saturation for the same value of σ_i. In the following section, we will show that this feature can improve tracking performance.

SIMULATION EXAMPLE AND COMPARISONS

To verify the effectiveness of the controller, we executed simulations for a 2-DOF (degree of freedom) direct-driven robot manipulator. The parameters are given as

$$\boldsymbol{M}=\begin{bmatrix}3.3+0.24\cos q_2 & 0.11+0.12\cos q_2\\ 0.11+0.12\cos q_2 & 0.11\end{bmatrix},$$

$$\boldsymbol{C}=\begin{bmatrix}-0.12\dot{q}_2\sin q_2 & -0.12(\dot{q}_1+\dot{q}_2)\sin q_2\\ 0.12\dot{q}_1\sin q_2 & 0\end{bmatrix},$$

$$\boldsymbol{G}=\begin{bmatrix}48.02\sin q_1+1.96\sin(q_1+q_2)\\ 1.96\sin(q_1+q_2)\end{bmatrix},$$

$$\boldsymbol{F}_{\mathrm{v}}=\mathrm{diag}\{2.5,\ 0.2\},\ \boldsymbol{U}=\mathrm{diag}\{500,\ 500\},$$

$$\tau_{1\mathrm{M}}=120\ \mathrm{N{\cdot}m},\ \tau_{2\mathrm{M}}=20\ \mathrm{N{\cdot}m},$$

and the desired position trajectories as

$$q_{\mathrm{d}1}(t)=\left[60(1-\mathrm{e}^{-3t^3})+20(1-\mathrm{e}^{-3t^3})\sin(6t)+5\right]\ (\mathrm{deg}),$$

$$q_{\mathrm{d}2}(t)=\left[75(1-\mathrm{e}^{-2t^3})+105(1-\mathrm{e}^{-2t^3})\sin(1.5t)+10\right]\ (\mathrm{deg}).$$

In practical situations, the initial position errors are not always 0. Controllers without saturation functions usually result in large initial torque inputs, which may even exceed the actuator torque limit. To evaluate the performance of the controller without loss of generality, the initial desired positions of each joint were set as 5° and 10°, respectively.

Firstly, we carried out some simulations on the proposed controller to see how the tracking performance varied with different error-gain matrices.

Tracking errors of each joint were as shown in Figs.2a and 2b, where the error-gain matrices were chosen as $\boldsymbol{K}_e$=$\boldsymbol{K}_\xi$=diag{2, 1}, diag{3, 2}, and diag{5, 1.5}, and $\boldsymbol{K}_{\mathrm{p}}$, $\boldsymbol{K}_{\mathrm{d}}$ were selected as diag{4.5, 4}, diag{1.5, 0.5} respectively, satisfying Eq.(16) by trial and error.

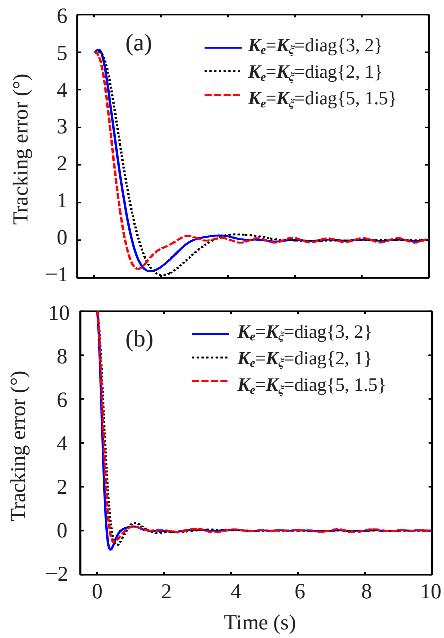

Fig.2 Tracking errors of (a) the 1st and (b) the 2nd joints

Generally, large error gains result in a large overshoot and oscillation. When error gains were too small, there was a long adjustment time. Because of the coupling relationship between the two joints of the robot, it is difficult to determine the strict rules between good tracking performance and the corresponding error-gain matrix. However, proper settings of the error gains can definitely benefit the tracking results.

We compared our controller Eq.(38) with the controllers proposed by Loria and Ortega (1995) (hereafter called L-O's, given in Eq.(39)) and Moreno-Valenzuela *et al*.(2008a) (hereafter called M-S-C's, given in Eq.(40)). The architectural comparison of the three controllers is shown in Table 1.

Table 1 Architectural comparison

Controller	Saturation function	Error-gain matrix
Ours	Has	Has
M-S-C's	Has	Has not
L-O's	Has not	Has not

The control law in L-O's is

$$\boldsymbol{\tau} = \boldsymbol{M}\ddot{\boldsymbol{q}}_{\mathrm{d}} + \boldsymbol{C}_{\mathrm{d}}\dot{\boldsymbol{q}}_{\mathrm{d}} + \boldsymbol{G} + \boldsymbol{F}_{\mathrm{v}}\dot{\boldsymbol{q}}_{\mathrm{d}} + \boldsymbol{K}_{\mathrm{p}}\boldsymbol{e} + \boldsymbol{K}_{\mathrm{d}}\boldsymbol{\xi}, \quad (39)$$

and the control law in M-S-C's can be written as

$$\boldsymbol{\tau} = \boldsymbol{M}\ddot{\boldsymbol{q}}_{\mathrm{d}} + \boldsymbol{C}_{\mathrm{d}}\dot{\boldsymbol{q}}_{\mathrm{d}} + \boldsymbol{G} + \boldsymbol{F}_{\mathrm{v}}\dot{\boldsymbol{q}}_{\mathrm{d}} + \boldsymbol{K}_{\mathrm{p}}\mathrm{Atan}(\boldsymbol{e}, \boldsymbol{I}) + \boldsymbol{K}_{\xi}\mathrm{Atan}(\boldsymbol{\xi}, \boldsymbol{I}), \quad (40)$$

where $\boldsymbol{e}$ and $\boldsymbol{\xi}$ in each controller have the same relationship as Eq.(13), and $\boldsymbol{I}\in\mathbb{R}^{n\times n}$ is the identity matrix.

To make fair comparisons, we selected the same proportional and derivative gains: $\boldsymbol{K}_{\mathrm{p}}$=diag{4.5, 4}, $\boldsymbol{K}_{\mathrm{d}}$=diag{1.5, 0.5}.

Our controller gave a satisfactory performance in the trajectory tracking, where we set $\boldsymbol{K}_{\boldsymbol{e}}$=diag{3, 2}, $\boldsymbol{K}_{\xi}$=diag{3, 2} (Figs.3a and 3b).

The comparisons of tracking errors are shown in Figs.4a and 4b, and the quantified comparisons using the standard criteria of adjusting time, overshoot, root mean square (RMS) value of the position tracking error computed on a trip of time T (10 s) are shown in Table 2. The adjusting time was defined as a period from the start to the moment the tracking error e_i just falls into the area of ±0.02° and RMS was defined as

$$\mathrm{RMS}[e_i(t)] = \sqrt{\frac{1}{T}\int_0^T |e_i(t)|^2 \mathrm{d}t}, \quad i=1, 2, \quad (41)$$

$$\mathrm{RMS}[\boldsymbol{e}(t)] = \sqrt{\frac{1}{T}\int_0^T \|\boldsymbol{e}(t)\|^2 \mathrm{d}t}. \quad (42)$$

Table 2 Performance comparison

Parameter		Value		
		Ours	M-S-C's	L-O's
Adjusting time (s)	1st joint	4.4	7.7	8.2
	2nd joint	1.6	3.3	4.1
Overshoot (°)	1st joint	0.83	0.93	0.76
	2nd joint	0.87	0.86	1.04
RMS (°)	e_1	1.174	1.515	1.324
	e_2	1.040	1.228	0.987
	$\|\|\boldsymbol{e}\|\|$	1.568	1.950	1.651

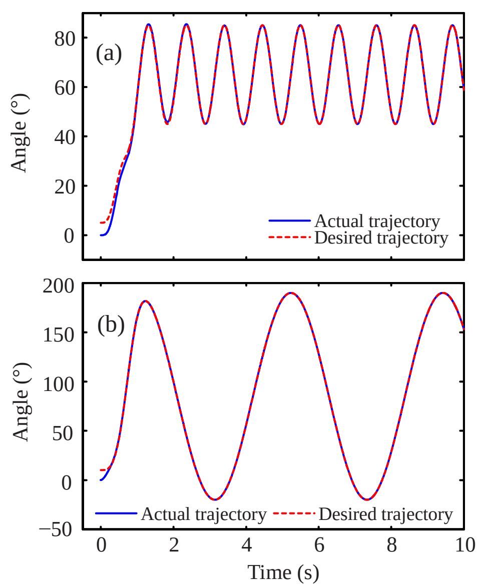

Fig.3 Trajectory tracking of (a) the 1st and (b) the 2nd joints

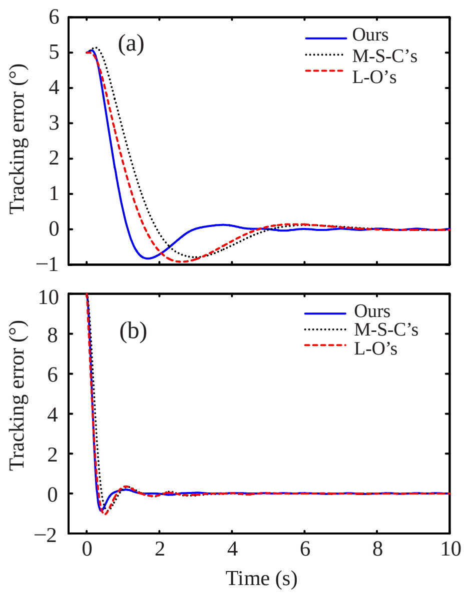

Fig.4 Comparison of (a) the 1st and (b) the 2nd joint tracking errors

Our controller had the shortest adjusting time, and a relatively small overshoot among the three controllers (Table 2). More importantly, it also gained the lowest value of RMS[$\boldsymbol{e}(t)$] and a relatively low RMS[$e_i(t)$] in each joint. That is because we chose a wider range saturation function—arctan incorporating an appropriate positive definite diagonal error-gain matrix for the control law.

Figs.5a and 5b show a comparison of torque inputs. The L-O controller presented rude transients. In particular, the second joint failed to respect the constraint τ_{2M}, giving a torque input of about 45 N·m rather than 20 N·m. The maximum absolute torque input value of each joint using our and M-S-C's controllers are practically the same, at about 80 and 5 N·m.

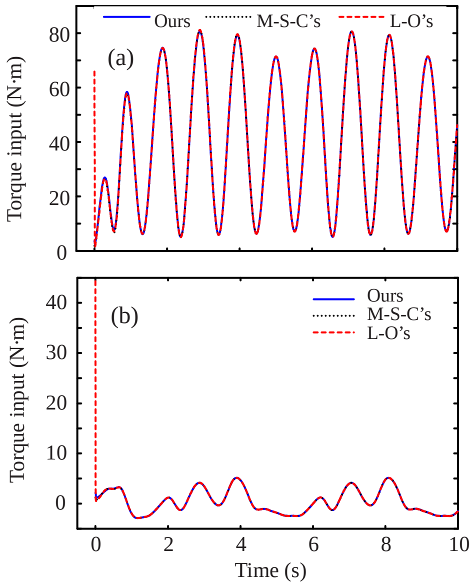

Fig.5 Comparison of (a) the 1st and (b) the 2nd joint torque inputs

CONCLUSION

The problem of torque outputs of joint actuators having upper bounds exists almost everywhere in the practical control of robot manipulators. To deal with it, we proposed a generalized tracking controller with bounded inputs based on stability theory of singularly perturbed systems. By applying the proper error-gain diagonal matrix to the arc tangent saturation function used in the control law, the sample controller designed by following the generalized scheme gave a better tracking performance with only position measurements than those without error-gain matrices or saturation functions. Theoretical analysis and simulation experiments verified the effectiveness of the proposed controller.

References

de Queiroz, M.S., Hu, J., Dawson, D.M., 1997. Adaptive position/force control of robot manipulators without velocity measurements: theory and experimentation. *IEEE Trans. Syst. Man Cybern. Part B*, **27**(5):796-809. [doi:10.1109/3477.623233]

Dixon, W.E., de Queiroz, M.S., Zhang, F., Dawson, D.M., 1999. Tracking control of robot manipulators with bounded torque inputs. *Robotica*, **17**(2):121-129. [doi:10.1017/S0263574799001228]

Kelly, R., Santibanez, V., Berghuis, H., 1997. Point-to-point robot control under actuator constraints. *Control Eng. Pract.*, **5**(11):1555-1562. [doi:10.1016/S0967-0661(97)10009-0]

Kelly, R., Santibanez, V., Loria, A., 2005. Control of Robot Manipulators in Joint Space. Springer-Verlag, Berlin, p.95-109.

Khalil, H.K., 2007. Nonlinear Systems (3rd Ed.). Publishing House of Electronics Industry, Beijing, p.456-459.

Laib, A., 2000. Adaptive output regulation of robot manipulators under actuator constraints. *IEEE Trans. Rob. Autom.*, **16**(1):29-35. [doi:10.1109/70.833185]

Loria, A., Nijmeijer, H., 1998. Bounded output feedback tracking control of full actuated Euler-Lagrange systems. *Syst. Control Lett.*, **33**(3):151-161. [doi:10.1016/S0167-6911(97)80170-3]

Loria, A., Ortega, R., 1995. On tracking control of rigid and flexible joints robots. *Appl. Math. Comput. Sci.*, **5**(2):101-113.

Moreno-Valenzuela, J., Santibanez, V., Campa, R., 2008a. A class of OFT controllers for torque-saturated robot manipulators: Lyapunov stability and experimental evaluation. *J. Intell. Rob. Syst.*, **51**(1):65-88. [doi:10.1007/s10846-007-9181-6]

Moreno-Valenzuela, J., Santibanez, V., Campa, R., 2008b. On output feedback tracking control of robot manipulators with bounded torque input. *Int. J. Control Autom. Syst.*, **6**(1):76-86.

Paden, B., Panja, R., 1988. Globally asymptotically stable PD+ controller for robot manipulators. *Int. J. Control*, **47**(6):1697-1712. [doi:10.1080/00207178808906130]

Reyes, F., Kelly, R., 2001. Experimental evaluation of model-based controllers on a direct-drive robot arm. *Mechatronics*, **11**(3):267-282. [doi:10.1016/S0957-4158(00)00008-8]

Santibanez, V., Kelly, R., 2001. Global Asymptotic Stability of Bounded Output Feedback Tracking Control for Robot Manipulators. Proc. 40th IEEE Conf. on Decision and Control, **2**:1378-1379. [doi:10.1109/.2001.981082]

Santibanez, V., Kelly, R., Reys, F., 1998. A new set-point controller with bounded torques for robot manipulators. *IEEE Trans. Ind. Electron.*, **45**(1):126-133. [doi:10.1109/41.661313]

Zavala-Rio, A., Santibanez, V., 2006. Simple extensions of the PD-with-gravity-compensation control law for robot manipulators with bounded inputs. *IEEE Trans. Control Syst. Technol.*, **14**(5):958-965. [doi:10.1109/TCST.2006.876932]